Int. J. Advanced Design and Manufacturing Technology, 2022, Vol. 15, No. 4, pp. 105-112

DOI: 10.30486/admt.2022.1962069.1363 *ISSN: 2252-0406* *https://admt.isfahan.iau.ir*

Fuzzy Tracking Control of the 3PRR Parallel Rehabilitation Robot

Moosarreza Shamsyeh Zahedi, Zahra Fathipour*
Department of Mathematics,
Payame Noor University, Tehran, Iran
E-mail: m.s.zahedi@pnu.ac.ir, Zahra.fathipour@yahoo.com
*Corresponding author

Majid Anjidani
Department of Computer Engineering and Information Technology,
Payame Noor University, Tehran, Iran
E-mail: M_anjidani@pnu.ac.ir

Received: 2 July 2022, Revised: 6 October 2022, Accepted: 12 October 2022

Abstract: In this study, a couple of 3PRR parallel robot is used for the rehabilitation process of a patient to eliminate a walking disability and leads to his treatment. The 3PRR robot has three degrees of freedom, provided by three prismatic actuators. Also using a couple of them, can quickly rehabilitate and provide the rehabilitation movements of a patient in the walking process. In this study, the extraction of kinematic and dynamic Equations of the robot was investigated, and a fuzzy-logic-based controller is performed. This controller has the ability to repel unwanted disturbances to follow the desired path. All modelling was simulated by MATLAB software. The simulation results show that using the mathematical model and controller, it is easy to go any desired path in the workspace; and this controller will be able to repel environmental disturbances like the sudden movement of patients.

Keywords: Fuzzy Tracking Control, Modeling, 3PRR Parallel Robot, Rehabilitation, Walking Operation

Biographical notes: Moosarreza Shamsyeh Zahedi received his PhD from the University of Pune-India in 2007 in the field of Applied Mathematics. He is now an assistant professor at PNU. More than 15 papers and 2 published books are the results of his research so far. His research interests include image processing and fractal application in biology. **Zahra Fathipour** is a PhD candidate at PNU in the field of Applied Mathematics. She received her MSc in Applied Mathematics from Kerman University in 2010. Her research interests include modelling dynamic systems, optimization, and control. **Majid Anjidani** received his PhD from IUST in 2017 in the field of Computer Engineering. His research interests include robotics, machine vision, machine learning, and virtual reality.

Research paper

1 INTRODUCTION

By definition, a stroke is the loss of brain function due to a disorder or blockage of a blood vessel. As a result, the damaged part of the brain cannot function normally, leading to the inability to move one or more limbs [1]. According to statistics, about eight hundred thousand people in the United States have a stroke each year, and only three hundred thousand people can survive after a stroke. This number reaches two million people in China every year. Even in Canada, 50,000 people have a stroke each year. After treatment, vital signs become stable; but brain damage is not reversible. Among the patients who survive, most patients develop mobility impairment for a long time [2]. According to the theory of brain flexibility, if patients are trained in rehabilitation for some time, part of the movement ability can be restored [3]. However, the recovery process is time-consuming; and it needs experienced therapists. As a result, the need to use a rehabilitation robot is well seen [4]. Since 1980, various types of robotic therapy devices have been studied in different countries [5]. For this reason, research on a rehabilitation robot was performed to correct the gait operations of a person with mobility impairments. The studied mechanism is shown in "Fig. 1". In this mechanism, two parallel robots with three degrees of freedom create the required gait pattern by moving the legs, while the body weight is supported by a restraint system. This design is based on previous studies [6-9] on the parameters of the footpath in human gait; it consists of three main movements: moving (vertical and horizontal), raising the leg, and lowering the leg, which must be considered and fully simulated.

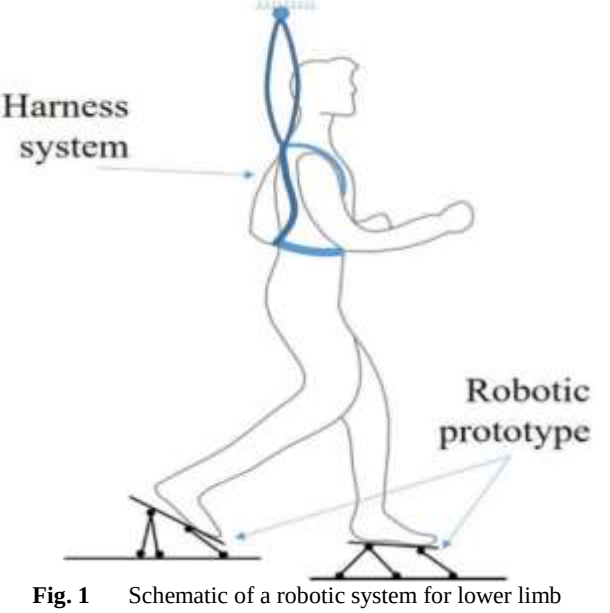

Fig. 1 Schematic of a robotic system for lower limb rehabilitation [9].

In this rehabilitation mechanism, each leg needs a parallel robot consisting of three linear actuators positioned in the same directions. The parallel robot is shown in "Fig. 2".

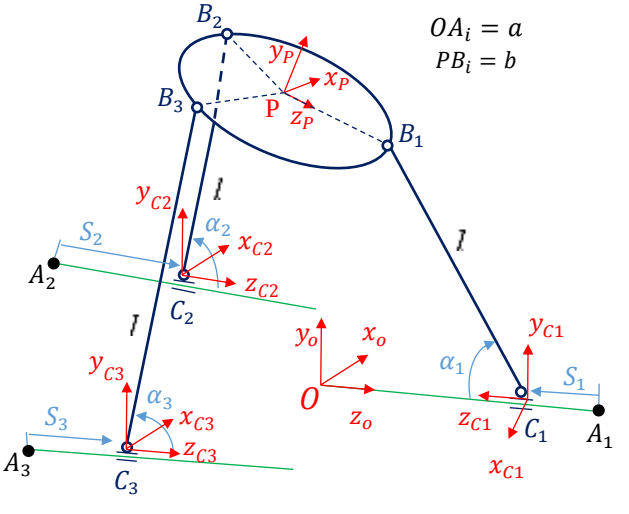

Fig. 2 Schematic of the 3PRR robot.

Each robot end-effector is supported by three links with passive and active prismatic joints. The movements of linear actuators create the required paths in the end-effector; which follows a pre-calculated gait pattern. The

training path can be achieved by combining three types of movements: 1- Transfer along the actuator axis while maintaining the direction and height of the footplate. This movement is achieved by moving all three actuators equally and in one direction. 2- It is possible to make net changes in the height of the end-effector by moving the same amount, in two parallel actuators in one direction and a third in the opposite direction. 3- Orientation of the end-effector by moving each of the actuators while the other is fixed; or it moves at different velocities, it is supplied. The exact path of rehabilitation depends on the age, weight, and height of the patient based on the type of injury or problem and the considerations of the physiotherapist. Parallel robots have been noted for their velocity, robustness, accuracy, and high loading capabilities.

One of the robots that can be considered as a kind of Stewart robot [10] as the most famous parallel robot is a robot with three degrees of freedom and the name 3PRR, which is considered in this study. The 3PRR robot has more freedom to move on the horizontal plane than the Stewart robot due to the presence of prismatic joints. The end-effector of this robot is connected to the prismatic joints with three links and does not have the problem of multiple links of the Stewart robot (6 links). As mentioned, not much research has been done on modelling and controlling this robot. The only case in which the robot has been modelled has focused on its structural optimization [9]. In other studies, on the 3PRR robot, the robot studied moved in two dimensions, which is different from the current spatial robot [11-16]; and the path of sliders was not similar to the robot under study [17-18].

For this reason, attention was paid to the research background of robots similar to the 3PRR spatial robot. One of the robots that are very similar to the robot is called 3PRS. In 2005, Li and Xu [19] proposed the exact solution of the inverse kinematics, and numerical solution forward kinematics, of the 3PRS robot. Then, its dynamic Equations were studied. In 2010, Tsai and Yuan performed an inverse dynamics analysis of the 3PRS robot by analysing the reaction forces acting on the joints and simulating it in a circular path [20]; in 2011, they solved its forward dynamics in the mentioned method and controlled it [21].

Then in 2014, they solved forward dynamics by taking into account the friction force [22]. In one of the latest studies, Tourajizadeh and Gholami modelled and optimally controlled the 3PRS robot [23]. They used the Lagrange method to model the robot. Their work will be the basis for modelling the present study [23-24]. The results of experimental and theoretical research indicate the fact that to control the motion of systems that have complex or nonlinear dynamics, the use of fuzzy controllers is a powerful tool [25]. In addition, the use of this type of controller can increase the robustness of the system to changes in environmental disturbances [26]. The proposed fuzzy controller tracks the desired path by overcoming the disturbances and tries to place the actuators in that path. In this regard, the fuzzy control of a parallel robot was performed [27]. The results of the movement of this robot indicate very good control of the robot and its acceptable velocity of movement.

In this paper, the kinematic and dynamic modeling of the 3PRR robot has been extracted by the Lagrange method, which according to the literature has not been similar and no research has been done in this field. Furthermore, the robust control of the 3PRR robot is modeled and implemented using the fuzzy fuzzy-logic inference, which is the most important innovation of this paper. The imbalance of the patient while using the rehabilitation robot, which causes the robot to experience external disturbances due to sudden movements, is the importance of implementing such a controller; and the necessity of such a controller seems vital.

For this purpose, a fuzzy controller was designed based on Mamdani inference. Using the obtained model and the controller designed for this parallel rehabilitation robot, the required path for rehabilitation of the patient's ankle in the presence of external force (patient weight) was well-traveled. In this paper, forward and inverse kinematics of the robots were extracted. Then, using the Lagrangian method, the dynamic Equations of the robot were obtained and after removing the Lagrangian coefficients, it was modelled in the form of state space. Then, the fuzzy controller was designed based on Mamdani's inference. Finally, all Equations obtained in MATLAB software were simulated and controlled.

2 KINEMATIC MODELING

Due to the similarity between 3PRR and 3PRS robots, the method used in [23] was used to model the 3PRR rehabilitation robot. As shown in "Fig. 2", point O is the origin of the reference coordinates and point A_i is the beginning of the prismatic rail.

$$o = \begin{bmatrix} 0 \\ 0 \\ 0 \end{bmatrix}, A_1 = \begin{bmatrix} 0 \\ 0 \\ a \end{bmatrix}, A_2 = \begin{bmatrix} b\frac{\sqrt{3}}{2} \\ 0 \\ -a \end{bmatrix}, A_3 = \begin{bmatrix} -b\frac{\sqrt{3}}{2} \\ 0 \\ -a \end{bmatrix}. \quad (1)$$

Where, a is the length of the prismatic joint rail. Denavit-Hartenberg method was used to select the coordinate systems and the link DH parameters extracted according to the [28] ("Table 1").

Table 1 DH parameters of the Links

Link	e	β	d	Θ
OC1	0	180	$a - s_1$	180
OC2	b	0	$-a + s_2$	0
OC3	-b	0	$-a + s_3$	0

Where, e (distance between the previous z-axis and the new z-axis along the new x-axis), β (angle between the previous z-axis and the new z-axis around the new x-axis), d (vertical distance between the origin of the previous coordinate and the new ones along the axis of the previous z), and Θ (the angle between the axes of the previous x and the new x around the axis of the previous z). The homogeneous transfer matrix according to the parameters of "Table 1" is as follows:

$$\begin{cases} H_{c_1}^{o} = R_{z,\theta_1} T_{z,d_1} T_{x,e_1} R_{x,\beta_1} \\ H_{c_2}^{o} = R_{z,\theta_2} T_{z,d_2} T_{x,e_2} R_{x,\beta_2} \\ H_{c_3}^{o} = R_{z,\theta_3} T_{z,d_3} T_{x,e_3} R_{x,\beta_3} \end{cases} \quad (2)$$

Where, $R_{z,\theta}$ is the rotation about the z-axis as much as θ and $T_{z,d}$ is the translations along the z-axis and is equal to d. The position of the B_i relative to the C_i local coordinate is:

$$B_i^{c_i} = \begin{bmatrix} 0 \\ l\ sin\alpha_i \\ l\ cos\alpha_i \end{bmatrix} \quad (3)$$

Where, l is the length of the links and α_i is the angle of the i[th] link connected to the C_i joint with its carrier rail. The position of point B_i in the reference coordinate connected to point O is as follows:

$$\begin{bmatrix} B_i^o \\ 1 \end{bmatrix}_{(s_i,\alpha_i)} = H_{c_i}^{o} \begin{bmatrix} B_i^{c_i} \\ 1 \end{bmatrix}, \qquad i = 1,2,3 \quad (4)$$

The rotation angles of the moving plane around the coordinate axes of the reference coordinate connected to the O point were considered as yaw, pitch, and roll, the final rotation matrix will be as follows:

$$R_{\varphi,\theta,\psi} = \begin{bmatrix} c\varphi c\theta & -s\varphi c\psi + c\varphi s\theta s\psi & s\varphi s\psi + c\varphi s\theta c\psi \\ s\varphi c\theta & c\varphi c\psi + s\varphi s\theta s\psi & -c\varphi s\psi + s\varphi s\theta c\psi \\ -s\theta & c\theta s\psi & c\theta c\psi \end{bmatrix} \quad (5)$$

Given the positions of the point $p = [x\ y\ z]^T$ we have:

$$[B_1^o \quad B_2^o \quad B_3^o]_{(x,y,z,\psi,\theta,\varphi)} = p[1 \quad 1 \quad 1] + R_{\varphi,\theta,\psi} \begin{bmatrix} 0 & \frac{b\sqrt{3}}{2} & \frac{-b\sqrt{3}}{2} \\ 0 & 0 & 0 \\ b & \frac{-b}{2} & \frac{-b}{2} \end{bmatrix} \quad (6)$$

Finally, the kinematic constraints of the robot, for use in system dynamics modeling, were obtained from the equality of the Equations (5) and (7) as follows:

$$\begin{bmatrix} f_1 \\ \vdots \\ f_9 \end{bmatrix} = \begin{bmatrix} B_1^o \\ B_2^o \\ B_3^o \end{bmatrix}_{(x,y,z,\psi,\theta,\varphi)} - \begin{bmatrix} B_1^o \\ B_2^o \\ B_3^o \end{bmatrix}_{(s_i,\alpha_i)} = 0 \quad (7)$$

3 DYNAMIC MODELING

The end-effector of the robot is circular, and the whole mass can be assumed at the center of the mass. To the modelling of the dynamics of the system, [x, y, z, ψ, θ, ϕ, α_1, α_2, α_3, S_1, S_2, S_3]^T were used as twelve generalized coordinates. The kinetic energy of the robot is equal to [29]:

$$\begin{cases} T_p = \frac{1}{2}\left(\omega_p^T I_p \omega_P + M V_p^T V_P\right) \\ T_l = \frac{1}{2}\sum_{i=1}^{3}\left(\omega_i^T I_{li} \omega_i + m V_i^T V_i\right) \end{cases}, T = T_p + T_l \quad (8)$$

T_p and M are the mass and energy of the end-effector. T_l and m are the mass and energy of the links. I_p is the moment of inertia of the end-effector and I_{li} is the moment of inertia of the i[th] link, and both rea relative to the reference coordinates. The moment of inertia of each link was written on the coordinate $(xyz)_{li}$ ((shown in "Fig. 3"); And to transfer it to the reference coordinate, the rotation matrix of these two coordinates was used relative to each other.

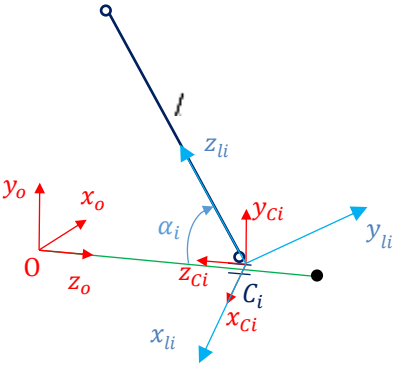

Fig. 3 Reference and local coordinates for calculating the moment of inertia of the links.

Also, the moment of inertia of the end-effector relative to the coordinate $(xyz)_p$ was written and taken to the reference coordinate. To calculate I_{li} and I_p can be written:

$$\begin{cases} I_p = \frac{1}{2} M b^2 R_{\varphi,\theta,\psi} \begin{bmatrix} 0.5 & 0 & 0 \\ 0 & 1 & 0 \\ 0 & 0 & 0.5 \end{bmatrix} R_{\varphi,\theta,\psi}^T, \\ I_{li} = \frac{1}{3} m l^2 R_{li}^o \begin{bmatrix} 1 & 0 & 0 \\ 0 & 1 & 0 \\ 0 & 0 & 0 \end{bmatrix} R_{li}^{oT}. \end{cases} \quad (9)$$

All velocities were written in the reference coordinate system:

$$\begin{cases} \omega_P = \begin{bmatrix} \dot{\psi} \\ \dot{\theta} \\ \dot{\phi} \end{bmatrix}, \quad v_P = \begin{bmatrix} \dot{x} \\ \dot{y} \\ \dot{z} \end{bmatrix}, \\ \omega_i = R_{Ci}^o \begin{bmatrix} -\dot{\alpha}_i \\ 0 \\ 0 \end{bmatrix}, \quad v_i = \frac{d}{dt} G_i . \\ G_i = H_{Ci}^o [0 \quad 0.5 l sin(\alpha_i) \quad 0.5 l cos(\alpha_i) \quad 1]^T \end{cases} \quad (10)$$

The potential energy of the robot is equal to:

$$U = Mgy + mg \frac{l}{2} \sum_{i=1}^{3} \sin(\alpha_i) \quad (11)$$

g is the acceleration of the earth's gravity. Lagrange's Equations of motion are equal to:

$$\begin{cases} \frac{d}{dt}\left(\frac{\partial L}{\partial \dot{q}_i}\right) - \frac{\partial L}{\partial q_i} + \sum_{k=1}^{9} \lambda_k \frac{\partial f_k}{\partial q_i} = Q_i \\ L = T - U \\ q = [x; y; z; \psi; \theta; \varphi; \alpha_1; \alpha_2; \alpha_3; s_1; s_2; s_3] \\ Q = [0; 0; 0; 0; 0; 0; 0; 0; 0; F_1; F_2; F_3] \end{cases} \quad (12)$$

Where, Q represents generalized forces. In this study, the friction force was negligible. f_k is the robot constraints obtained from Equation (7).

$$\begin{cases} \frac{d}{dt}\left(\frac{\partial L}{\partial \dot{q}_i}\right) = \frac{\partial}{\partial \dot{q}_j}\left(\frac{\partial L}{\partial \dot{q}_i}\right) \ddot{q}_j + \frac{\partial}{\partial q_j}\left(\frac{\partial L}{\partial \dot{q}_i}\right) \dot{q}_j, \\ \frac{\partial}{\partial \dot{q}_j}\left(\frac{\partial L}{\partial \dot{q}_i}\right) = m_{ji}, \quad \frac{\partial}{\partial q_j}\left(\frac{\partial L}{\partial \dot{q}_i}\right) = c_{ji}, \\ \frac{\partial L}{\partial q_i} = g_i, \quad \frac{\partial f_k}{\partial q_i} = a_{ki}. \end{cases} \quad (13)$$

Finally, the Equation of motion will be equal to:

$$M\ddot{q} + C\dot{q} - G + A^T \lambda = Q \quad (14)$$

Where, M is the inertia matrix, C is the Coriolis matrix, G is the gravity vector, A is the weight matrix of Lagrangian coefficients, and Q is the generalized force vector. To eliminate the Lagrangian coefficients from the Equation of motion, the null-space of the matrix A was obtained from the following definition [30]:

$$\begin{cases} AS = 0, \\ \vec{v} = [\dot{s}_1; \dot{s}_2; \dot{s}_3], \\ \dot{\vec{q}} = S\vec{v}, \\ \ddot{\vec{q}} = \dot{S}\vec{v} + S\dot{\vec{v}}. \end{cases} \quad (15)$$

Where, S is the null-space matrix. Multiplying S^T from the left in Equation (14) and placing the derivatives q of Equation 15 will give:

$$S^T M S\dot{\vec{v}} + S^T M \dot{S}\vec{v} + S^T C S\vec{v} - S^T G = S^T Q \quad (16)$$

Where, $S^T Q = \vec{F} = [F_1; F_2; F_3]$. To calculate the derivative of the null-space matrix, we can write:

$$\begin{cases} AS = 0 \rightarrow \dot{A}S + A\dot{S} = 0 \rightarrow \dot{S} = -A^{-1}\dot{A}S \\ A^{-1} = A^T (AA^T)^{-1} \end{cases} \quad (17)$$

By selecting $\vec{X}_{6\times1} = [S_1, S_2, S_3, v^T]^{\mathrm{T}}$ as the state space variables, the system state space form is equal to:

$$\begin{cases} \dot{\vec{X}} = \begin{bmatrix} \vec{v} \\ \dot{\vec{v}} \end{bmatrix} = \begin{bmatrix} \vec{v} \\ h \end{bmatrix} + \begin{bmatrix} [0]_{3\times3} \\ (S^T M S)^{-1} \end{bmatrix} \vec{F}, \\ h = (S^T M S)^{-1} S^T \left(G - C S\vec{v} - M\dot{S}\vec{v}\right). \end{cases} \quad (18)$$

4 CONTROLLER DESIGN

Fuzzy controllers have acceptable efficiency and performance in controlling the movement of robots as well as performing special maneuvers. One way to design a fuzzy controller is to break down complex system behaviors into multiple movements within the robot. After designing a suitable control algorithm for each section, their corresponding actions can be combined. In this paper, the fuzzy controller is designed in such a way that it can track the desired path well by determining the appropriate control force and has good resistance to initial disturbances. This controller is designed according to the if-then rules in the following form:

If s_i is A and $\dot{s}_i$ is B, then u_i is C (19)

The "and" and "or" operators are defined as follows:

$$\begin{aligned} \mu_{A\cup B} &= max(\mu_A(u), \mu_B(u)) \\ \mu_{A\cap B} &= min(\mu_A(u), \mu_B(u)) \\ \mu_{A\cup B} &= max(\mu_A(u), \mu_B(u)) \\ \mu_{A\cap B} &= min(\mu_A(u), \mu_B(u)) \end{aligned} \quad (20)$$

In the proposed controller, Mamdani fuzzy inference system was used along with the defuzzification method of the centroid. In the first step, the fuzzy controller, after receiving the inputs, performs the fuzzification process, then combines the membership functions based on

Mamdani inference using the fuzzy operator. In the next step, the values of the membership functions combine and the outputs are defuzzification. The input of the fuzzy system was selected as an error and its derivative of the desired value at a given time. The membership functions of these inputs were considered Gaussian functions. Position and velocity errors of the robot were selected as five functions [-2 -1 0 +1 +2], where the range of the changes between [-1 1]. This selection is a general case and a coefficient is assigned to the system error to change the velocity and position error range. For the output of the fuzzy system, which is the same control force required for the robot to move in the path, according to the Mamdani method, the membership functions of these outputs were considered Gaussian functions. Finally, a representation of the fuzzy system inputs and outputs is shown in "Fig. 4".

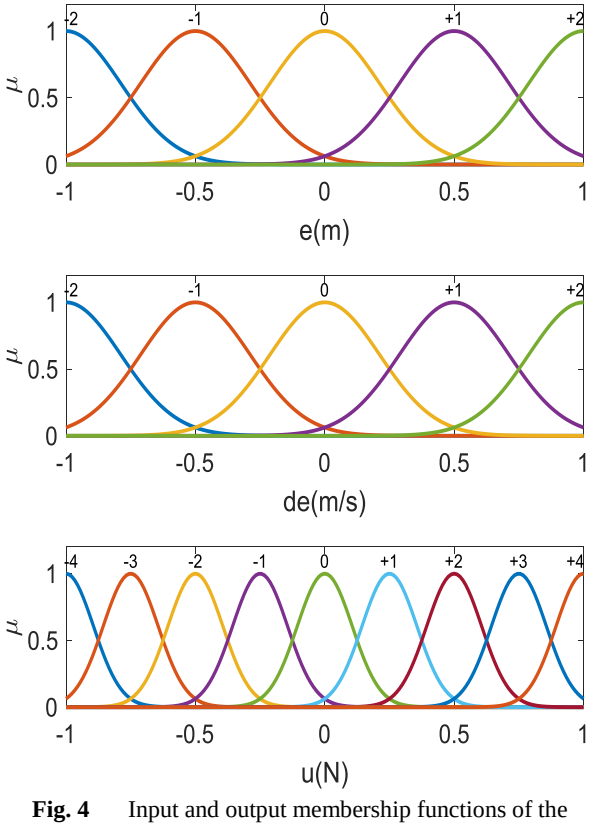

Fig. 4 Input and output membership functions of the Mamdani fuzzy system.

A set of fuzzy rules was chosen to extract the appropriate control force in "Table 2".

5 SIMULATION RESULTS

In this research, after the kinematic and dynamic modelling of the 3PRR rehabilitation robot, a designed controller was applied to the dynamic model. For this purpose, Equation (18) was used as the system. The values in Table 3 were used for simulation.

Table 2 Fuzzy Rules

Number	Fuzzy rules					
1	If "e" is	-2	and "de" is	-2	then "u" is	+4
2		-2		-1		+3
3		-2		0		+2
4		-2		+1		+1
5		-2		+2		0
6		-1		-2		+3
7		-1		-1		+2
8		-1		0		+1
9		-1		+1		0
10		-1		+2		-1
11		0		-2		+2
12		0		-1		+1
13		0		0		0
14		0		+1		-1
15		0		+2		-2
16		+1		-2		+1
17		+1		-1		0
18		+1		0		-1
19		+1		+1		-2
20		+1		+2		-3
21		+2		-2		0
22		+2		-1		-1
23		+2		0		-2
24		+2		+1		-3
25		+2		+2		-4

Table 3 Value of robot parameters

Parameter	symbol	Unit	value
Jacks' course	a	(m)	0.8
Radius of the moving platform	b	(m)	0.2
Length of the links	l	(m)	0.5
Mass of the moving platform	M	(kg)	1
Mass of the links	m	(kg)	0.1
Gravitational acceleration	g	(m/s2)	9.8

Due to the nature of the robot rehabilitation, the angle of the end-effector (φ) around the x-axis was considered as a sine wave with an amplitude of 20 degrees (0.35 rad). During this movement, the other angles of the end-effector should remain zero. Also, the motion of the end-effector in the directions x and z should be constant and zero. Such a move is desirable and will meet all rehabilitation needs. According to the expressed movement needs, and considering the inverse kinematic simulation, the movement path of the robot sliders is considered as follows, and was used to simulate the performance of the fuzzy controller in the tracking operation.

$$\begin{cases} s_1 = -0.05 - 0.42sin(t) \\ s_2 = 0.6 - 0.42sin(t) \\ s_3 = -0.3 + 0.42sin(t) \end{cases} \quad (21)$$

To bring the control scenario as close as possible to the real state, an external force of 20 N was applied to the end-effector in the opposite direction of the y-axis. This force can be equated to the condition in which an 80 N-weight patient enters the robot during a rehabilitation operation (half of the patient's weight will be borne by the harness system). The control force was determined using a fuzzy system designed and applying the existing rules in "Table 2" to the position and velocity error of the intended path and is applied to the robot prismatic actuators. The position and velocity of these actuators are shown in "Fig. 5".

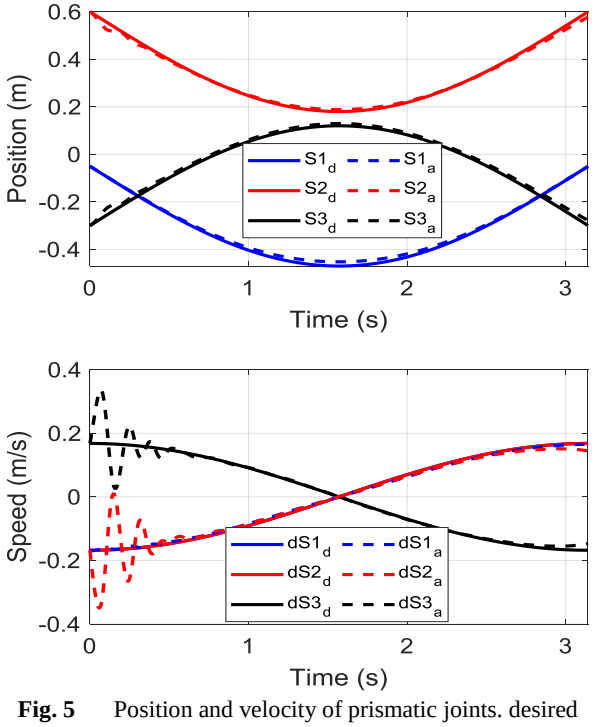

Fig. 5 Position and velocity of prismatic joints. desired path (d), the path taken by the controller (a).

As shown in the figure above, the fuzzy controller has been able to track the path required for rehabilitation and has followed it well. The application of an external force initially causes a small error in the position of the prismatic actuators, but fuzzy control has corrected this error by applying appropriate oscillations to the velocity of the sliders. The control forces applied to each prismatic actuator are shown in "Fig. 6".

As it turns out, the control force is applied uniformly and smoothly, and is well able to handle external loads (patient weight). The smoothness of the applied control force indicates the capability of the implemented controller. In addition, the minimum-maximum control force is obtained smoothly and the direction of force is gently sloping. This is very important in the use of control instruments and prevents possible breakdowns in the drive motors.

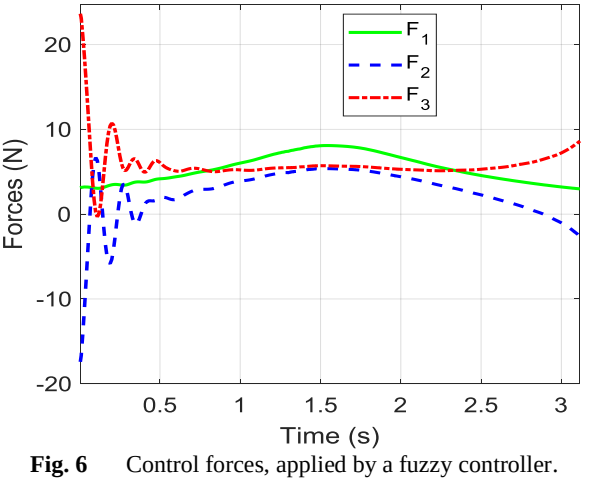

Fig. 6 Control forces, applied by a fuzzy controller.

6 CONCLUSIONS

In this study, kinematic and dynamic analysis of the 3PRR rehabilitation robot was performed and robot Equations of motions were obtained by the Lagrange method. Finally, robot control in tracking operations was performed without using system dynamic Equations and only using fuzzy logic. For this purpose, a fuzzy controller was designed based on Mamdani's inference. Using the obtained model and the controller designed for this parallel rehabilitation robot, the required path for rehabilitation of the patient's ankle in the presence of external force (patient weight) was well-traveled. During this operation, the tracking error is less than 3% and the applied control force has good smoothness and a gentle slope.

REFERENCES

[1] Wolfe, C. D., The Impact of Stroke, British Medical Bulletin, Vol. 56, No. 2, 2000, pp. 275-286.

[2] Tyson, S. F., Hanley, M., Chillala, J., Selley, A., and Tallis, R. C., Balance Disability After Stroke, Physical Therapy, Vol. 86, No. 1, 2006, pp. 30-38.

[3] French, B., Thomas, L. H., Leathley, M. J., Sutton, C. J., McAdam, J., Forster, A., and Watkins, C. L., Does Repetitive Task Training Improve Functional Activity After Stroke? A Cochrane Systematic Review and Meta-Analysis, Journal of Rehabilitation Medicine, Vol. 42, No. 1, 2010, pp. 9-15.

[4] Wang, M., Design and Analysis of an Adjustable Wrist Rehabilitation Robot, 2014: (PhD Thesis).

[5] Siciliano, B., Khatib, O., Force Control, Luigi Villani, Joris De Schutter, Springer handbook of robotics. Springer-Verlag Berlin Heidelberg, 2008.

[6] Mariani, B., Hoskovec, C., Rochat, S., Büla, C., Penders, and J., Aminian, K., 3D Gait Assessment in Young and Elderly Subjects Using Foot-Worn Inertial Sensors, Journal of Biomechanics, Vol. 43, No. 15, 2010, pp. 2999-3006.

[7] Dadashi, F., Mariani, B., Rochat, S., Büla, C. J., Santos-Eggimann, B., and Aminian, K., Gait and Foot Clearance Parameters Obtained Using Shoe-Worn Inertial Sensors in a Large-Population Sample of Older Adults, Sensors, Vol. 14, No. 1, 2014, pp. 443-457.

[8] Zhang, C., Lan, B., Matsuura, D., Mougenot, C., Sugahara, Y., and Takeda, Y., Kinematic Design of a Footplate Drive Mechanism Using a 3-DOF Parallel Mechanism for Walking Rehabilitation Coordinate, Journal of Advanced Mechanical Design, Systems, and Manufacturing, Vol. 12, No. 1, 2018, pp. JAMDSM0017-JAMDSM0017.

[9] Valdez, S. I., Gutierrez-Carmona, I., Keshtkar, S., and Hernandez, E. E., Kinematic and Dynamic Design and Optimization of a Parallel Rehabilitation Robot, Intelligent Service Robotics, Vol. 13, No. 3, 2020, pp. 365-378.

[10] Stewart, D., A Platform with Six Degrees of Freedom, Proceedings of the Institution of Mechanical Engineers, Vol. 180, No. 1, 1965, pp. 371-386.

[11] Caro, S., Chablat, D., Ur-Rehman, R., Wenger, P., Multiobjective Design Optimization of 3–Prr Planar Parallel Manipulators, in Global Product Development : Springer, 2011, pp. 373-383.

[12] Javid, G., Akbarzadeh, M. R., Akbarzadeh, A., Nabavi, S. N., Trajectory Tracking of 3-PRR Parallel Manipulator with PI Adaptive Fuzzy Terminal Prismatic Mode Controller, 1st International E-Conference on Computer and Knowledge Engineering (ICCKE), 2011, pp. 156-161: IEEE.

[13] Si, G., Chu, M., Zhang, Z., Li, H., and Zhang, X., Integrating Dynamics into Design and Motion Optimization of a 3-PRR Planar Parallel Manipulator with Discrete Time Transfer Matrix Method, Mathematical Problems in Engineering, Vol. 1, No.1, 2020, pp. 126-131.

[14] Staicu, S., Inverse Dynamics of the 3-PRR Planar Parallel Robot, Robotics and Autonomous Systems, Vol. 57, No. 5, 2009, pp. 556-563.

[15] Zhang, X., Mills, J. K., Cleghorn, W. L., Effect of Axial Forces on Lateral Stiffness of a Flexible 3-PRR Parallel Manipulator Moving with High-Velocity, in 2008 International Conference on Information and Automation, 2008, pp. 1458-1463: IEEE.

[16] Zhao, B., Zhang, X., Zhan, Z., Wu, Q., and Zhang, H., Multi-scale Graph-guided Convolutional Network with Node Attention for Intelligent Health State Diagnosis of a 3-PRR Planar Parallel Manipulator, IEEE Transactions on Industrial Electronics, Vol. 1, No. 1, 2021, pp. 556-563.

[17] Kumar, P., Sudheer, A., Workspace Optimization of 3PRR Parallel manipulator for drilling operation using Genetic Algorithm, in Proceedings of the Advances in Robotics, 2017, pp. 1-5.

[18] Selvakumar, A. A., Karthik, K., Kumar, A., Sivaramakrishnan, R., and Kalaichelvan, K., Kinematic and Singularity Analysis of 3 PRR Parallel Manipulator, in Advanced Materials Research, Vol. 403, 2012, pp. 5015-5021.

[19] Li, Y., Xu, Q., Kinematics and Inverse Dynamics Analysis for a General 3-PRS Spatial Parallel Mechanism, Robotica, Vol. 23, No. 02, 2005, pp. 219-229.

[20] Tsai, M. S., Yuan, W. H., Inverse Dynamics Analysis for a 3-PRS Parallel Mechanism Based on a Special Decomposition of The Reaction Forces, Mechanism and Machine Theory, Vol. 45, No. 11, 2010, pp. 1491-1508.

[21] Tsai, M. S., Yuan, W. H., Dynamic Modeling and Decentralized Control of a 3 PRS Parallel Mechanism Based on Constrained Robotic Analysis, Journal of Intelligent & Robotic Systems, Vol. 63, No. 3-4, 2011, pp. 525-545.

[22] Yuan, W. H., Tsai, M. S., A Novel Approach for Forward Dynamic Analysis of 3-PRS Parallel Manipulator with Consideration of Friction Effect, Robotics and Computer-Integrated Manufacturing, Vol. 30, No. 3, 2014, pp. 315-325.

[23] Tourajizadeh, H., Gholami, O., Optimal Control and Path Planning of a 3PRS Robot Using Indirect Variation Algorithm, Robotica, Vol. 38, No. 5, 2020, pp. 903-924.

[24] Tourajizadeh, H., Gholami, O., A New Optimal Method for Calculating the Null Space of a Robot using NOC Algorithm; Application on Parallel 3PRS Robot, ADMT Journal, Vol. 13, No. 1, 2020, pp. 1-15.

[25] Azarafza, R., Mohammadhoseni, S., and Farrokhi, M., Free Chattering Fuzzy Sliding Mode Controllers to Robotic Tracking Problem, ADMT Journal, Vol. 5, No. 2, 2012.

[26] Ghafouri, M., Daneshmand, S., Design and Evaluation of an Optimal Fuzzy Pid Controller for an Active Vehicle Suspension System, Transactions of Famena, Vol. 41, No. 2, 2017, pp. 29-44.

[27] Vermeiren, L., Dequidt, A., Afroun, M., Guerra, and T. M., Motion Control of Planar Parallel Robot Using the Fuzzy Descriptor System Approach, ISA Transactions, Vol. 51, No. 5, 2012, pp. 596-608.

[28] Spong, M. W., Hutchinson, S., Vidyasagar, M., Robot Modeling and Control, Jon Wiley & Sons, Inc., ISBN-100-471-649, 2005.

[29] Jazar, R. N., Advanced Dynamics: Rigid Body, Multibody, and Aerospace Applications, John Wiley & Sons, 2011.

[30] Liang C., M. Lance, G., A Differentiable Null Space Method for Constrained Dynamic Analysis, Journal of Mechanisms, Transmissions, and Automation in Design, Vol. 109, No. 3, 1987, pp. 405-411.